Molecular Vibrations (McGraw-Hill, New York, 1955), Appendix X, pp. 312-340.

[6]J. Murphy, H. H. Caspers, and R. A. Buchanan, J. Chem. Phys. 40, 743 (1964); D. F. Hornig, J. Chem. Phys. 16, 1063 (1948).

[7]The samples were obtained from the National Museum of Natural History, Smithsonian Institution, Washington, D. C. (specimens Nos. R402, 91779, and C288).

[8]The primitive vectors in the basal plane are chosen to be perpendicular to the sides of the hexagon.

[9]J. A. Wilson and A. D. Yoffe, Advan. Phys. 18, 193 (1969).

DYNAMIC PROTON POLARIZATION IN AlK AND Al(NH_4) ALUM*

Philip J. Bendt

Los Alamos Scientific Laboratory, University of California, Los Alamos, New Mexico 87544

(Received 18 June 1970)

Over 50% proton polarization has been attained in three sulfate alum crystals containing dilute Cr^{3+} ions, at 1 K and ~19.5 kG, with limited microwave power (~$\frac{1}{4}$ W). The EPR spectra are dominated by the $(-\frac{1}{2},\frac{1}{2})$ transition, with linewidths varying from 10 to 22 G. Al(NH_4) alum should make useful polarized proton targets because it contains 1.97 times as much hydrogen by weight as lanthanum magnesium nitrate.

In $AlK(SO_4)_2\cdot 12H_2O$ and $Al(NH_4)(SO_4)_2\cdot 12H_2O$, each Al ion is surrounded by six water molecules forming a regular octahedron, with an Al-H_2O separation of about 2 Å.[1] If a small fraction (<0.5%) of the diamagnetic Al is replaced with paramagnetic Cr^{3+} ions, the paramagnetic ions are dipolar-coupled with the protons, forming a system suitable for dynamic proton polarization by the "solid effect."[2] We have studied the EPR spectra, relaxation times, and dynamic proton polarization in four alum crystals, along with a lanthanum magnesium nitrate (LMN) crystal for comparison.[3]

Though Cr^{3+} has a spin $S=\frac{3}{2}$, the EPR spectra are dominated by the $(-\frac{1}{2},\frac{1}{2})$ transition, especially when the (111) plane is oriented perpendicular to the magnetic field H (see Fig. 1). An explanation of this was given by Bleaney,[4] who suggested that the zero-field Stark splitting is not quite constant throughout the mixed crystal; this smears out the EPR lines, except for the $(-\frac{1}{2},\frac{1}{2})$ transition. The theoretical EPR spectra[5] can still be identified at 1.3 K in AlK alum, and from the spectra of crystal No. 1 we measured the zero-field splitting $2D$, obtaining 332 MHz, corresponding to 0.011 cm^{-1}. We were also able to measure the hyperfine coupling constant $|A|$ for Cr^{53}, obtaining $(1.6\pm0.05)\times10^{-3}$ cm^{-1}.[6] Details of the EPR results are contained in an article to be submitted elsehwere.

The values of p_{max} in Table I are the maximum (negative) proton polarizations we measured, and are limited by the microwave power delivered to the cavity (190 ± 290 mW).[7] Since the allowed and "forbidden" EPR transitions are sufficiently well separated (30 G) that only the tails of the EPR lines overlap,[8] the theory of dynamic polarization in dipolar crystals by Jeffries[9] and Borghini[10] applies. The steady-state polarization is given by

$$p_s = \frac{P_0}{(1+f)(1+S_{1/2}/S)}, \tag{1}$$

where P_0 is the thermal equilibrium polarization of the ions,[11] f is the leakage factor, S is the EPR saturation factor, and $S_{1/2}$ is a constant which depends on the crystal properties and the magnetic field. S was determined from the cavity Q (~2000) and the microwave power. The polarization grows in with a single time constant τ,

$$p(t)=p_s(1-e^{-t/\tau}). \tag{2}$$

We determine both p_s and τ from polarization

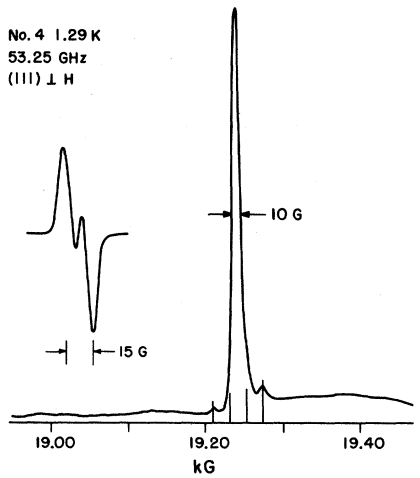

FIG. 1. The EPR spectrum of Al(NH_4) alum crystal No. 4 with the (111) planes perpendicular to the magnetic field. The positions of the four Cr^{53} hyperfine lines are indicated. The derivative of the proton NMR line, at −44% polarization, is shown as an insert.

Table I. Properties of the crystals, conditions during dynamic proton polarization, and the measurements.

	AlK No.1	AlK No.2	Al(NH_4)No.3	Al(NH_4)No.4	LMN
Weight (mg)	460	501	330	290	357
Al:Cr ratio	435	215	380	590	100[a]
Cr ions/cm^3 ($\times 10^{18}$)	5.14	10.39	5.73	3.69	15.8[b]
EPR line width (G)	20	15	22	10	6
T_{1e} at 0.96 K (ms)	2.5	2.0	3.0	2.8	11.5
T_{1p} at 0.93 K (s)	13,000	3,950	3,350	1,350	1,320
Polarization conditions:					
Temperature (K)	1.00	1.00	1.02	1.02	1.00
Magnetic field (G)	18,932	19,575	19,553	19,593	19,598
Microwave freq. (GHZ)	52.40	54.18	54.12	54.23	74.08
Microwave power (mW)	190	190	290	260	200
Microwave field (mG)	84	84	102	97	73
p_{max} (- %)	54	43	53	51	77
p_s (- %)	64	50	58	55	80
τ (minutes)	90	53	23	19	10
Leakage factor, f	0.0020	0.0026	0.0095	0.034	0.021
Saturation[c], S	31	32	50	92	480
$S_{\frac{1}{2}}$	11	23	23	47	79
B	1.16	1.39	1.09	1.48	1.30
Experimental r_1 (Å)	5.5	6.4	4.4	3.6	5.3

[a]The nominal La:Nd ratio.
[b]Nd ions/cm^3 ($\times 10^{18}$).
[c]$S = T_{1e}T_{2e}(\gamma_e H_{1e})^2$, where γ_e is the ion gyromagnetic ratio and H_{1e} is the microwave field, given above. T_{2e} was calculated from the EPR linewidth.

growth curves, three of which are shown in Fig. 2. The value of τ is given by[9]

$$\tau = T_{1p}[1 + S/S_{1/2}(1+f)]^{-1}, \quad (3)$$

where T_{1p} is the proton relaxation time. Dropping the factors $(1+f)$ which equal ~1, Eqs. (1) and (3) can be combined to obtain

$$\tau/T_{1p} + p_s/P_0 = B, \quad (4)$$

where the theoretical value $B = 1$ apparently assumes that the magnetic resonance is perfectly tuned; experimentally $B > 1$.

The ratio σ of the forbidden to allowed transition rates is given by[9]

$$\sigma = \left(\frac{2}{S_{1/2}}\right)\left(\frac{T_{1e}}{T_{1p}}\right)\frac{1}{(1+f)} = \frac{3}{10}\left(\frac{g\beta}{H}\right)^2 \frac{1}{r_1^3 r_2^3}, \quad (5)$$

where T_{1e} is the ion relaxation time, g is the ion g factor,[12] and β is a Bohr magneton. The radii r_1 and r_2 refer to the shell-of-influence model,[9] in which $r_2 = (4\pi N/3)^{-1/3}$ (N is the number of paramagnetic ions per unit volume), and r_1 is the distance between an ion and the closest protons. Because of the local magnetic field of the ions, the resonant frequency of the closest protons is more than a linewidth away from that of the majority of the protons, so the closest protons are not pumped by the microwaves. This justifies replacing the crystallographic ion-proton separation with a larger radius. We suggest that r_1 should be considered a parameter determined by experiment. We have used p_s from the polarization growth curves and Eqs. (1) and (5) to calculate experimental values for r_1. The ac-

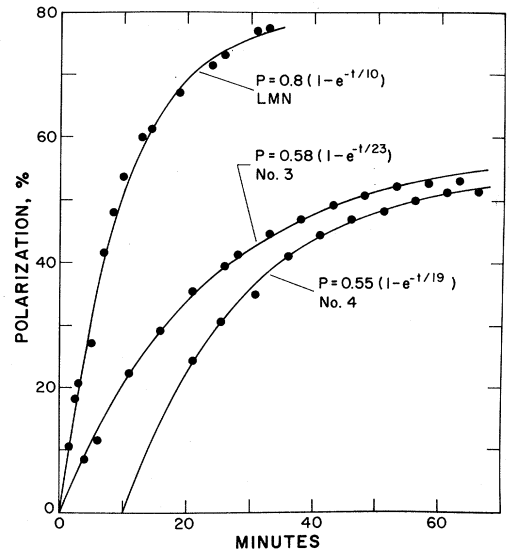

FIG. 2. Polarization growth rate curves for LMN and Al(NH_4) alum crystals No. 3 and No. 4. All polarizations shown are negative and the growth rate constant is given in minutes. The solid lines fit the equations given.

curacy of the measurements and the ability of the theory to give consistent results with different crystal parameters is indicated by the variation in the values of B and r_1 in Table I. Both p_s and $1/\tau$ would be larger with more microwave power.

The long T_{1e} for LMN contributes to the large value of S, and indicates that the ion spin-lattice relaxation in LMN is more strongly "phonon bottlenecked" than in the alum. The long T_{1p} for AlK alum No. 1 is responsible for the 90-min value of τ and apparently results from higher purity. From measurements of T_{1p} on this crystal at 0.93, 1.17, and 1.46 K, we estimate that T_{1p} may be about 3 days at 0.5 K, where Gunter and Jeffries[9] measured 40 h for LMN (at 19.5 kG). Such a long relaxation time would make pure AlK alum very useful for "storing" proton polarization.

In considering the utility of alum crystals for polarized-proton targets, we point out that they have the advantage of a higher hydrogen density by weight than LMN, by a factor of 1.6 for AlK alum and 1.97 for Al(NH_4) alum. LMN requires less microwave power and has a larger P_0 in a given magnetic field. At a high magnetic field (26 kG), and using a high-power microwave oscillator,[13] these advantages will provide only 5% additional polarization in LMN, while using Al(NH_4) alum will expose approximately twice the number of polarized protons to the beam for the same charged-particle energy loss. If the alum has any advantage over the recently developed hydrocarbon targets,[14] it results from the convenience of handling a solid crystal at room temperature, the reliability of using a crystal whose performance has been measured before it is put in the beam, and the simplicity of a target system that does not require cooling with liquid ^{3}He.

We thank Dr. J. E. Simmons, Dr. J. A. Jackson, and Mr. J. C. Martin for assistance with equipment used for the measurements.

---

*Work performed under the auspices of the U. S. Atomic Energy Commission.

[1]R. W. G. Wyckoff, *Crystal Structures* (Interscience, New York, 1951), 2nd Ed., Vol. 3.

[2]A. Abragam and M. Borghini, in *Progress in Low Temperature Physics*, edited by C. J. Gorter (North-Holland, Amsterdam, 1964), Vol. IV, Chap. VIII; C. D. Jeffries, *Dynamic Nuclear Orientation* (Interscience, New York, 1963).

[3]The LMN crystal was grown by the late Dr. T. R. Roberts. A nominal 1% of the La was replaced with "unenriched" Nd. The presence of some Nd nuclei with magnetic moments may account for the short proton relaxation time.

[4]B. Bleaney, Proc. Roy. Soc., London, Ser. A 204, 203 (1950).

[5]P. R. Weiss, Phys. Rev. 73, 470 (1948); C. Kittel and J. M. Luttinger, Phys. Rev. 73, 162 (1948); C. A. Whitmer, R. T. Weidner, J. S. Hsiang, and P. R. Weiss, Phys. Rev. 74, 1478 (1948); D. M. S. Bagguley and J. H. E. Griffiths, Proc. Roy. Soc., London, Ser. A 204, 188 (1950).

[6]Bleaney and Bowers measure $|A| = (1.85 \pm 0.1) \times 10^{-3}$ cm^{-1} for Cr^{53}; see B. Bleaney and K. D. Bowers, Proc. Phys. Soc., London A64, 1135 (1951).

[7]Microwave power was measured by the boiloff rate from the helium bath.

[8]The full width at half-power of the EPR lines varied from 10 to 22 G; the widths of the proton NMR lines varied from 7 to 15 G. The proton line shapes did not change as the polarization increased.

[9]C. D. Jeffries, Univ. of California, Berkeley, Technical Report No. UCB-34P20-T-1 (unpublished); T. J. Schmugge and C. D. Jeffries, Phys. Rev. 138, A1785 (1965); T. E. Gunter and C. D. Jeffries, Phys. Rev. 159, 290 (1967).

[10]M. Borghini, Phys. Rev. Lett. 16, 318 (1966).

[11]At 1 K and 19.5 kG, P_0 equals 0.86 for Cr^{3+} in alum and 0.94 for Nd^{3+} in LMN.

[12]The g factor for Cr^{3+} in alum is independent of crystal orientation and equals 1.977. For Nd^{3+} in LMN, the g factor has a maximum value of 2.70 with the c axis perpendicular to the magnetic field.

[13]Available from Varian of Canada and Thomson-

CSF Electron Tubes.
[14]S. Mango, Ö. Runolfsson, and M. Borghini, Nucl. Instrum. Methods 72, 45 (1969); D. A. Hill, J. B. Ketterson, R. C. Miller, A. Moretti, R. C. Niemann, L. R. Windmiller, A. Yokosawa, and C. F. Hwang, Phys. Rev. Lett. 23, 460 (1969); A. Masaike, H. Glattli, J. Ezratty, and A. Malinovski, Phys. Lett. 30A, 63 (1969).

PRESSURE-INDUCED METAL-SEMICONDUCTOR TRANSITION AND 4*f* ELECTRON DELOCALIZATION IN SmTe

A. Jayaraman, V. Narayanamurti, E. Bucher, and R. G. Maines
Bell Telephone Laboratories, Murray Hill, New Jersey 07974
(Received 24 June 1970)

The pressure variation of resistivity and optical absorption in SmTe has been studied. A continuous pressure-induced semiconductor-to-metal transition is observed, which we ascribe to the promotion of electrons from the 4*f* level into the conduction band as the gap between them shrinks with pressure and finally vanishes. The gap deduced from the saturation resistivity ratio $\rho(P)_{sat}/\rho(0)$ is in good agreement with the gap of 0.62 ± 0.02 eV obtained from infrared absorption data.

The monochalcogenides of Sm, Eu and Yb crystallize in the NaCl structure[1] and are found to be semiconductors.[2,3] Because of their interest as magnetic semiconductors the Eu chalcogenides have received the most attention in recent years and quite extensive optical absorption measurements[4] and some pressure work[5,6] have been reported on them. Similar studies are conspicuously absent in the case of Sm and Yb compounds. This Letter reports the discovery of a continuous pressure-induced transition in SmTe from semiconducting to the metallic state, as the pressure is increased from 0 to 55 kbar. We ascribe this semiconductor-to-metal transition to the promotion of electrons from the 4*f* level into the conduction band as the gap between them shrinks with pressure and finally vanishes. The energy gap deduced from resistivity measurements is good agreement with our optical absorption data. We believe that the pressure behavior described for SmTe will prove to be the general pattern for the semiconducting rare-earth monochalcogenides.

Samarium telluride was prepared by reacting Sm metal chips in Te vapor at about 900°C for 48 h and subsequently melting the sample in a tantalum tube. The ingot thus obtained was polycrystalline, with fairly large-sized single crystals. The NaCl structure[1] and the lattice constant appropriate to SmTe were verified from the powder x-ray diffraction data. For resistivity measurements, single-crystal samples were cut from selected regions in the ingot. Ohmic contacts were provided with indium and the standard four-probe technique was used to measure the resistance. The room-temperature resistivity was approximately 10^3 Ω cm. For optical absorption studies, a polished single-crystal plate approximately 15 mm^2 in area and 0.1 mm in thickness was used.

High-pressure resistivity measurements were carried out under hydrostatic conditions up to about 45 kbar using *n*-pentane–isoamyl alcohol mixture as pressure medium, and up to 55 kbar using AgCl as pressure medium, in a piston-cylinder device. The two sets of measurements were in good agreement in the region of their overlap. The data on resistivity versus pressure are reproduced in Fig. 1. It will be seen that the resistivity decreases by almost seven orders of magnitude and saturates at about 55 kbar. The logarithm of resistivity versus pressure exhibits two straight-line regions, with a break in slope at about 20 kbar. The pressure coefficients $d\ln\rho/dp$ are −0.10 and −0.46 $kbar^{-1}$. These slopes yield -2.6×10^{-3} and -11.9×10^{-3} eV/kbar for the pressure coefficient of the carrier activation energy. At low pressures the temperature coefficient of resistivity is strongly negative and varies strongly with pressure. At the highest pressure it becomes positive, showing thereby metallic behavior.

Figure 2 shows the optical absorption as a function of photon energy. The principal absorption edge is centered at about 0.62 ± 0.02 eV (~2 μm). There is a subsidiary absorption at longer wavelengths centered at about 3 μm (0.38 eV). A weak absorption band centered at 0.22 eV (~5.6 μm) with a half-width of 0.02 eV was also observed (not shown in Fig. 2) in our scanning between 5 and 15 μm.

In order to explain the resistivity and optical